Diagrammatic methods for studying elementary excitations in thin magnetic films

1998 J. Phys.: Condens. Matter 10 7823

(http://iopscience.iop.org/0953-8984/10/35/014)

J. Phys.: Condens. Matter **10** (1998) 7823–7834. Printed in the UK PII: S0953-8984(98)78660-6

Diagrammatic methods for studying elementary excitations in thin magnetic films

S P Dias† and F A Oliveira‡

International Centre of Condensed Matter Physics and Instituto de Física, Universidade de Brasilia, 70919-970 Brasilia DF, Brazil

Received 14 October 1996, in final form 30 April 1998

Abstract. In this work we discuss a diagrammatic method for studying the long-wavelength magnetic excitation in an antiferromagnetic thin film. Although we examine this particular system, the method is quite general. We pay special attention to the modes localized at the surface in the absence of an applied static external field. Such modes are more symmetrical and more stable. There are two main results from this work. First, we transform the boundary condition into an abstract virtual potential which is used here to construct the Green's function for the elementary excitation in a film for a realistic situation. Second, we use such functions to obtain the surface dispersion relations and the power spectra of the modes. Numerical applications are demonstrated for MnF_2 thin films.

1. Introduction

It is very common in physics for the boundary conditions and constraints to be separated from the equations of motion. This way of thinking is desirable in most of the cases. However, in certain circumstances we may be able to transform a boundary condition into a potential; the great advantage of doing this is that one can then easily sum all contributions. Here, we study this possibility for a very specific problem.

The modes that we will discuss here are those which result from the coupling between the long-wavelength magnetic excitations and the electromagnetic field in an insulating antiferromagnetic film. Surface modes of this kind were first investigated by Hartstein *et al* [1] for semi-infinite ferromagnetic media. They found two different modes, one for each propagation direction. Later, Karsono and Tilley [2] recovered the reciprocity for finite geometry. Camley and Mills [3] and Fukui *et al* [4] carried out ATR (attenuated total reflection) studies for such modes. However, the investigations were concerned with dispersion relations, and very little has been said about the stability of the modes. In previous work [5, 6], we discussed the stability of the surface modes at the interface of a semi-infinite ferromagnet and we concluded that only the main (lower) branch was stable [6]. There we ensured the stability of the modes by requiring the power spectrum to be positive. Since a particular excitation may not exist for given values of the frequency, wavevector, and damping, it will appear in the power spectrum as zero or a negative number. Consequently, it becomes obvious that it is not just the dispersion relations that are needed to reach a conclusion as regards the stability of the modes: a full calculation of the power spectra

† E-mail: sandra@iccmp.br.
‡ E-mail: fao@iccmp.br.

0953-8984/98/357823+12$19.50

is also essential. However, to obtain the power spectra, we need to compute a response function, which in most cases is time consuming and onerous.

Recently [7], we formulated a method for constructing the Green's function for a film from the Green's function of a semi-infinite medium. The main idea is to transform the boundary condition at the interface into a virtual potential and, using diagrammatic methods similar to those used in quantum field theory and many-body theory [8], to sum all of the diagrams. Linear response theory has been used before for elementary excitations by authors such as Dobrzynski [9], and Sarmento and Tilley [10].

Maradudin and Zierau [11] and Stamps and Camley [12] have constructed surface response functions for antiferromagnets and applied them in a perturbation expansion for rough surfaces.

The main difference between these methods and ours is the idea of using a boundary condition as a virtual potential, which can be expanded in a series.

In section 2 we derive the Green's functions for the semi-infinite medium. In section 3 we use the diagrammatic method to obtain the Green's functions for the film, which are then used in section 4 to obtain analytical results for the power spectra and to perform some numerical applications for a MnF_2 film at zero field. Our conclusions are in given section 5.

2. Semi-infinite antiferromagnets

In this section we discuss the Green's functions for a semi-infinite antiferromagnet. For future use, we shall define the geometry as that of figure 1. The media 1 and 3 are neutral; they have no major effect on the magnetic excitations that we want to study. Medium 2 ($0 < x < -L$) is magnetic. For points close to $x = 0$, and for large L, this system may be seen as a semi-infinite one, for which the response function is simpler. From the semi-infinite response functions, we obtain (section 3) the Green's function for the thin film.

Since reciprocal propagation yields more stable modes, we expect also that modes which are more symmetrical will be more stable. On the other hand, we know that magnetic modes coupled with electromagnetic ones exist only over very narrow regions. Indeed, we shall see in section 4 that the interval over which the modes are stable is considerably smaller than that obtained from the usual definition of the dispersion relation. For the sake of simplicity, we pay particular attention to the zero-field regime. In that case, the tensor permeability $\boldsymbol{\mu}(\omega)$ is a diagonal even function of the frequency ω, given by

$$\boldsymbol{\mu}(\omega) = \begin{pmatrix} \mu_{xx} & 0 & 0 \\ 0 & \mu_{xx} & 0 \\ 0 & 0 & \mu_{zz} \end{pmatrix} \tag{1}$$

where $\mu_{zz} = \mu_0$ and

$$\mu_{xx} = \mu_0\left(1 + \frac{2\omega_m\omega_a}{\omega_0^2 - \omega^2}\right). \tag{2}$$

Here μ_0 is the magnetic permeability of the vacuum, and

$$\omega_0^2 = \omega_a^2 + 2\omega_a\omega_e \qquad \omega_m = 4\pi\gamma M \qquad \omega_a = \gamma H_A$$

where H_A is the anisotropic field, and ω_e the exchange frequency $\omega_e = \gamma H_{ez}$, with H_{ez} the z-component of the exchange field H_e. Using ϵ as the dielectric constant for medium 2, the wavevectors for the elementary excitations are

$$q_1^2 = q_{1x}^2 + Q_y^2 = \frac{\omega^2}{c^2} \tag{3}$$

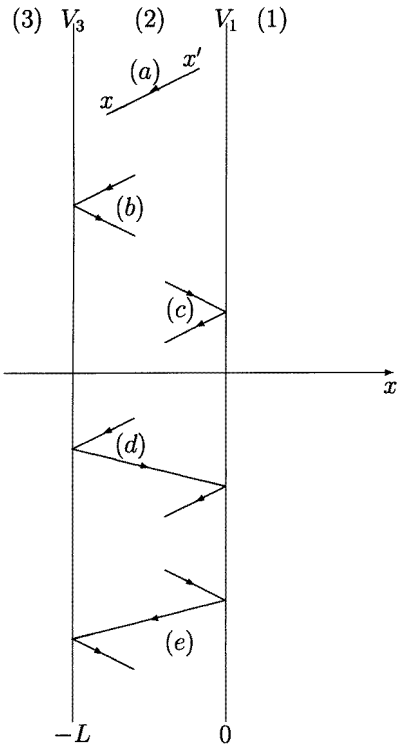

Figure 1. Basic diagrams for the elementary excitations in a film: (*a*) free propagation; (*b*), (*c*) propagation involving only one surface; (*d*), (*e*) propagation involving two surfaces.

$$q_2^2 = q_{2x}^2 + Q_y^2 = \epsilon\mu_{xx}\frac{\omega^2}{c^2}. \tag{4}$$

Since the breaking of the translational symmetry of the excitations occurs only in the x-direction, the wavevectors Q_y are the same for the two media. As the excitations have rotational symmetry in the zy-plane, we choose $Q_z = 0$ without lost of generality. Medium 1 only causes the decay of the surface excitations, while the spectra of medium 2 also involve volumetric excitations. We are now interested in obtaining the response of the magnetization $\boldsymbol{m}(\boldsymbol{r})$ due to an external field $\boldsymbol{h}$, which, for further use, is defined, in the long-range limit [25], as

$$\boldsymbol{h}(\boldsymbol{r}, t) = \boldsymbol{h}_0 \mathrm{e}^{\mathrm{i}(\boldsymbol{Q}\cdot\boldsymbol{r}-\omega t)}\delta(x - x').$$

From the wave equation of the magnetic field and the equations

$$\boldsymbol{m}(\boldsymbol{r}, t) = \boldsymbol{\chi}\boldsymbol{h}^{ext} \tag{5}$$

$$\boldsymbol{\Gamma} = \frac{1}{4\Pi}\boldsymbol{\chi}^{-1} = \begin{pmatrix} \Gamma_{xx} & 0 & 0 \\ 0 & \Gamma_{yy} & 0 \\ 0 & 0 & \Gamma_{zz} \end{pmatrix} \tag{6}$$

we obtain the magnetization equation (see [6, 13] and references therein)

$$\nabla^2(\boldsymbol{\Gamma}\boldsymbol{m}(\boldsymbol{r})) + \boldsymbol{\nabla}(\boldsymbol{\nabla}\cdot\boldsymbol{m}(\boldsymbol{r})) + \frac{\epsilon\mu_0\omega^2}{c^2}(\boldsymbol{\Gamma} + \mathbf{I})\boldsymbol{m}(\boldsymbol{r}) = D(\omega)\boldsymbol{h}(\boldsymbol{r}) \tag{7}$$

where $\boldsymbol{r}$ is the Cartesian coordinate, $\mathbf{I}$ is the identity matrix, and

$$D(\omega) = \frac{1}{4\pi}\left(\frac{\epsilon\mu_0\omega^2}{c^2} - q^2\right). \tag{8}$$

Solving this equation by the Green's function method [1, 7, 23, 24], we obtain

$$m_\alpha(r) = \int G_{\alpha,\beta}(r, r')D(\omega)h_\beta(r')\ \mathrm{d}r' \tag{9}$$

where $G(r, r')$ is the Green's function. The Greek indices α, β refer to the Cartesian components x, y. The relevant direction is the 'x'-direction. So, after some algebra, we can cast the result in the compact form

$$G_{\alpha\beta}(x, x') = A_{\alpha\beta}\left[B_{\alpha\beta}\mathrm{e}^{-\mathrm{i}q_{2x}|x-x'|} + \frac{\gamma^+}{\gamma^-}\eta_\alpha\mathrm{e}^{\mathrm{i}q_{2x}(x+x')}\right] \tag{10}$$

where

$$\gamma^\pm = q_{2x} \pm \mu_{xx}q_{1x} \tag{11}$$

$$A_{\alpha\beta} = \frac{q_2^2\delta_{\alpha\beta} - q_{2\alpha}q_{2\beta}}{2q_{2x}\mu_{xx}} \tag{12}$$

$$B_{\alpha\beta} = \delta_{\alpha,\beta} + (1 - \delta_{\alpha,\beta})\,\mathrm{sgn}(x - x') \tag{13}$$

$$\mathrm{sgn}(x - x') = \begin{cases} 1 & x > x' \\ -1 & x < x' \\ 0 & x = x' \end{cases} \tag{14}$$

$$\eta_\alpha = \begin{cases} -1 & \alpha = x \\ 1 & \alpha = y. \end{cases} \tag{15}$$

The first term of equation (10) has translational symmetry, while the second, which represents the surface contribution, does not. Although it has lost its translational symmetry, the Green's function has exchange symmetry for $x' \to x$. We shall present a more detailed discussion of the physics for the film Green's function in section 4.

3. The diagrammatic method

We now turn our attention to the central part of this work. We will obtain the Green's function for the magnetic excitations in thin films.

For excitation propagation, the main information about the character of the surface comes from the boundary conditions at the interfaces. Those conditions are frequently in terms of the fields and not in terms of the potential. Consequently, it becomes difficult to associate a Hamiltonian with simple phenomena, such as light or phonon reflection at a boundary. However, we have pointed out [7] a situation where one may put the two concepts together. Our starting point is observing that the number of components of a film Green's function is finite. Indeed, all five possible components are represented diagrammatically in figure 1. In particular, observe figure 1(a) and figure 1(c) and their corresponding terms in equation (10). For propagation which does not involve an interface, we shall consider the free propagator

$$G_0(x, x') = \mathrm{e}^{-\mathrm{i}q_{2x}|x-x'|}. \tag{16}$$

We drop the polarization factor $A_{\alpha,\beta}$ and the reference to Cartesian components, in view of the fact that the procedure is the same for all of them. We associate with the interface 2–1 a potential V_1 and with the interface 2–3 the potential V_3. For our case with $V_1 = V_3$, we retain both V_1 and V_3 in order to make our diagrams clearer. With the free propagator and the potentials V_1 and V_3, we can construct all of the Green's functions; for example

$$G_1(x, x') = G_0(x, 0)V_1G_0(0, x') = V_1 e^{iq_{2x}(x+x')}. \tag{17}$$

Equation (17) reproduces the second term of equation (10) with

$$V_1 = \frac{\gamma^+}{\gamma^-}. \tag{18}$$

All of the diagrams of figure 1 can be obtained in the same way. The full Green's function for the elementary excitations in the film is the sum of all possible propagations going from x' to x, so we have

$$\begin{aligned} G(x, x') = {} & G_0(x, x') + G_0(x, 0)V_1G_0(0, x') + G_0(x, 0)V_1G_0(0, -L)V_3G_0(-L, x') \\ & + G_0(x, 0)V_1G_0(0, -L)V_3G_0(-L, 0)V_1G_0(0, x') + \cdots \\ & + G_0(x, -L)V_3G_0(-L, x') + G_0(x, -L)V_3G_0(-L, 0)V_1G_0(-L, x') \\ & + G_0(x, -L)V_3G_0(-L, 0)V_1G_0(0, -L)V_3G_0(-L, x') + \cdots. \end{aligned} \tag{19}$$

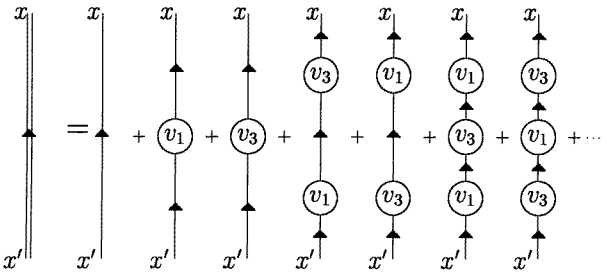

Figure 2. Feynman diagrams for the elementary excitations in thin film. The virtual potentials V_1 and V_3 are summed to all orders of interaction.

These contributions are represented diagrammatically in figure 2. Observe that a double-reflection propagation which returns to the same point will produce the factor

$$p = G_0(x, 0)V_1G_0(0, -L)V_3G_0(-L, x) = V_1V_3e^{-2iq_{2x}L} \tag{20}$$

which is just a constant. This means that it does not depend on the position. To extend our analogy with the diagrammatic methods in many-body theory, we define the generalized dielectric constant as the inverse of the sum of all possible closed trajectories; thus

$$\Sigma(Q_y, \omega) = (1 + p + p^2 + \cdots)^{-1} = 1 - V_1V_3e^{-2iq_{2x}L}. \tag{21}$$

Consequently, equation (19) becomes

$$G(x, x') = G_0 + (G_1 + G_3 + G_{13} + G_{31})/\Sigma(Q_y, \omega). \tag{22}$$

Finally, the last result with the proper polarization may be cast in the form

$$\begin{aligned} G_{\alpha\beta}(x, x') = {} & \frac{q_2^2\delta_{\alpha,\beta} - q_{2\alpha}q_{2\beta}}{2q_{2x}\mu_{xx}}\big[B_{\alpha\beta}e^{-iq_{2x}|x-x'|} \\ & + \Delta^{-1}\gamma^-[\gamma^+(\eta_\alpha e^{iq_{2x}(x+x')} + \eta_\beta e^{-iq_{2x}(2L+x+x')}) \\ & + \gamma^-(e^{iq_{2x}(x-x'-2L)} + \eta_\alpha\eta_\beta e^{iq_{2x}(x'-x-2L)})]\big] \end{aligned} \tag{23}$$

with

$$\Delta = (\gamma^{-})^2 \Sigma(Q_y, \omega). \tag{24}$$

We observe that the full Green's function is the sum of the bare Green's functions represented in figure 1 divided by the function $\Sigma(Q_y, \omega)$. So, the sum of all closed trajectories has the same screening effect as in an electron gas [8, 15, 16] where a bare potential $1/r$ may end up as the screened potential e^{-qr}/r, for example.

Equation (23) was obtained in a very general way using the information from equation (18) and free-propagator equation (16); no more information is needed. Although we are concerned here with retarded magnetic excitations, the results are not restricted to any particular type of excitation. These results have two main consequences: first, they avoid a large part of the calculations on going from a single interface to a film, i.e., from the knowledge of equation (18) we write down equation (23) immediately; second, they show up the similarity, mainly as regards the wave character, between many kinds of different excitation such as magnons, phonons, excitons, polarons, and polaritons. This latter result may be obtained from the poles of our Green's functions or from the zeros of our generalized dielectric function $\Sigma(Q_y, \omega)$.

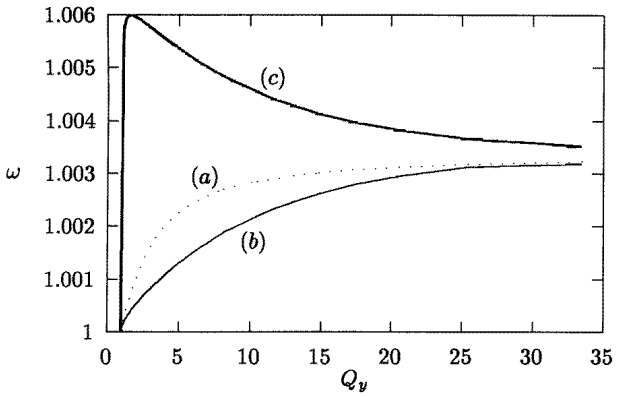

Figure 3. Dispersion relations for the surface modes in MnF_2. Here the frequencies are in units of the bulk magnon frequency ω_0, the wavevector is in units of $K_0 = c/\omega_0$, and the length is in units of $L_0 = K_0^{-1}$. Curve (a) is the mode for $L \to \infty$. Curve (b) is the lower mode for $L = 0.1$. Curve (c) is the highest mode for $L = 0.1$.

The first benefit of our method is that we obtain the dispersion relation equation (24); it may be obtained by using different methods, but the result that we have presented here is more elegant, simple, and efficient. Considering medium 1 and 3 as identical, equation (24) yields for the surface modes ($q_{2x} = -i\alpha$, $\alpha > 0$, $q_{1x} = i\beta$, $\beta > 0$)

$$q_{1x}\mu_{xx} = q_{2x} \tanh(iq_{2x}L/2) \tag{25}$$

and

$$q_{1x}\mu_{xx} = q_{2x} \coth(iq_{2x}L/2). \tag{26}$$

Equations (25) and (26) represent modes with high and low energy, relative to the single interface. They have even and odd symmetry with respect to a central plane in medium 2; see equation (23). Equations (25) and (26) are similar to those for the ground state and the first excited state of a quantum system, and reflect the wave character of the modes. These characteristics have been pointed out for phonons [14, 17, 18] and magnetic modes

[6, 13, 19, 20]. For real q_{2x}, we also obtained the guide modes [21]. For $L \to \infty$, the interaction between the surfaces becomes negligible, and equation (25) and equation (26) coalesce to the same form: $\gamma^- = 0$. In this limit, equation (25) and equation (26) reduce to

$$Q_y^2 = \frac{\mu_{xx}\omega^2(\epsilon - \mu_{xx})}{c^2(1 - \mu_{xx}^2)}. \tag{27}$$

In figure 3 we plot the dispersion relation for an unsupported MnF_2 film. The frequencies are given in units of $\omega_0 = 93.3$, while the wavenumber is given in units of $K_0 = \omega_0/c$ and the length in units of $L_0 = K_0^{-1}$. We use the parameters $\omega_a = 7.54$ kOe, $\omega_m = 7.85$ kOe, $\omega_e = 550$ kOe, $L_0 = 91$ μm. However, since our frequencies are given in relative units, the forms of the graphs are not affected by a 'bad' measure of those parameters. Curve (a) is for $L \to \infty$; curves (b) and (c) are for $L = 0.1$. Curve (b) represents the low-mode equation (26), while curve (c), equation (25), represents the high-mode equation. Observe that for $Q_y \to \infty$ ($e^{-iq_{2x}L} \to 0$), all of the curves converge to the same value:

$$\omega_s = \sqrt{2\omega_m\omega_a\mu_0/(1 + \mu_0) + \omega_0^2} = 1.0036.$$

We noticed that the splittings of the modes are similar to those of two hydrogen atoms put together, where a single level is split into two orbitals with even and odd spatial symmetry.

4. Power spectra

Now we turn our attention to the study of the power spectra of the magnetic modes. The dispersion relation gives us the primary information about the modes. However, it is not sufficient to describe them. We will define the region of the positive power spectrum as stable. Before we present the results, we first put the calculations in context by discussing the nature of the Green's functions that we have just obtained. The dispersion relation obtained in the last section could easily be obtained by using other methods [2, 5, 13, 18, 22–25], but this is not true of the Green's functions. Using the methods developed here, we reproduce various Green's functions obtained in the literature by direct calculation. In this way we get results for acoustic phonons [18], phonon–polaritons [14], phonon–excitons [25], surface magnetostatic modes in ferromagnets [19], antiferromagnets in the exchange-dominated regime [20], and retarded magnons in both ferromagnetic [13] and antiferromagnetic [6] systems.

The Green's function equation (23) was built up in such way as to obey the symmetry $G(x, x') = G(x', x)$. However, once the proper polarization is introduced into equation (23), the resulting equations for all of the components $G_{\alpha,\beta}$ obey

$$G_{\alpha,\beta}(x, x') = \pi_{\alpha,\beta}G_{\beta,\alpha}(x', x) \tag{28}$$

as required by time-reversal symmetry [22]. Here $\pi_{\alpha\alpha} = 1$, and the off-diagonal term $\pi_{\alpha,\beta}$ assumes the following values: 1, for variables which do not change sign under time reversal; and -1, for variables which do change sign [22]. We lose the translational symmetry, but, on the other hand, there is an exchange symmetry, i.e., the Green's function is no longer a function of $|x - x'|$, but, for x and x' in the same medium, $G_{\alpha\beta}(x, x')$ is invariant under the exchange of x and x'. This symmetry for thin films was observed by Loudon [18] for the phonon case, and demonstrated in [22] for a general case. The proof uses two basic arguments: linear response theory and time-reversal symmetry. On the other hand, the diagrammatic procedure developed here shows symmetry by direct construction.

This symmetry is very important in the discussion of some experiments—such as when considering selection rules for light scattering (see [22] and references therein).

For x and x' in different media, the symmetry relations (28) do not hold in a simple way. The reason for this is clear: on moving from one medium to another, the changes are no longer linear. Thus, the susceptibility, the dielectric constant, and the wavevector, change abruptly. Consequently, not all trajectories going from one medium to another are reversible; there may be instabilities and forbidden regions. The simplest example is as follows: one may always shine a ray of light from air onto water; however, the reverse procedure is not always possible, since total reflection may occur. For that prohibited region, the power spectrum will involve negative numbers.

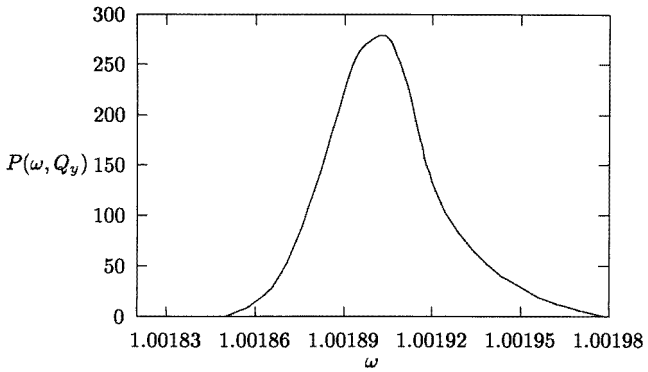

Figure 4. The maximum of the power spectrum as a function of the resonance frequencies ω. $P(\omega, q(\omega))$ is a function of ω, and $L = 0.1$.

Now that our Green's function is well defined, the power spectra may be readily obtained by using the fluctuation-dissipation theorem [6, 14]:

$$P(\omega, Q_y, x) = \frac{\hbar}{\pi}(n(\omega) + 1)\,\mathrm{Im}[G_{xx}(x, x') + G_{yy}(x, x')]\big|_{x=x'} \tag{29}$$

with $n(\omega)$ as the Bose–Einstein factor. As we are considering zero static external field, the x- and y-modes are not coupled. Thus the power spectra of the excitations depend only on G_{xx} and G_{yy}. Equation (29) gives a full description of the power spectrum as a function of ω, Q_y, and x. We take the dissipation into account by making $\omega = \omega + \mathrm{i}\Gamma$ ($\Gamma \ll \omega_0$) in equation (29). Choosing for every ω the form $\omega = \omega(Q_y)$, we get the maximum of the power spectrum in terms of ω. We get the maximum energy possible for all of the points of a dispersion relation, similar to that of figure 3. In figure 4 we plot the maximum of the power spectrum as a function of $\omega = \omega(Q_y)$. We use $L = 0.1$, and the dispersion relation of curve (b) of figure 3. We use $x = 0$, so we are at the interface 1–2. Similar results hold for the interface 2–3. We notice that the real modes are confined to a region smaller than that defined by the dispersion relation. Since we are working here with the maximum allowed power spectrum, we can see that there are no modes outside this range. That is, they are unstable outside of this region.

In figure 5 we plot the power spectrum as a function of Q_y. We select $\omega = 1.0019$ (which corresponds to the maximum value of P from figure 4). This is a more common experimental situation, where, for example, one has a fixed source of light and changes Q_y by changing the scattering angle. Figure 5 shows a very large value of P for $Q_y \approx 8$ which is a very active polariton region—i.e., the region where these modes are most probably found.

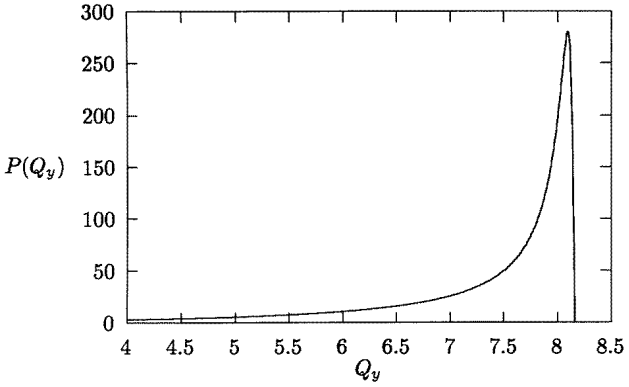

Figure 5. The power spectrum as a function of Q_y. We use $\omega = 1.0019$ and $L = 0.1$. For a very thin film the first peak is far away from the second one, and lies outside our range.

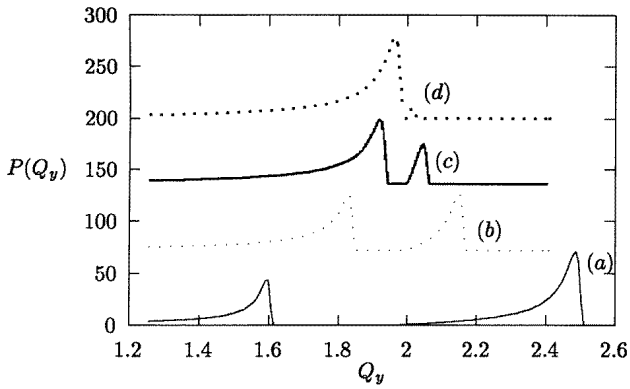

Figure 6. The power spectrum as a function of Q_y. Here $\omega = 1.002$. The curves are for the following values: (*a*) $L = 0.5$; (*b*) $L = 0.75$; (*c*) $L = 0.98$; (*d*) $L = 1.2$. The background is given by the straight part of the spectrum. We notice that as L increases, the modes converge to a single one.

In figure 6 we plot the power spectrum as a function of the wavenumber Q_y, for various thickness of the film. Here, also, $x = 0$ and $\omega = 1.002$. The curves are for the following values: (*a*) $L = 0.5$; (*b*) $L = 0.75$; (*c*) $L = 0.98$; (*d*) $L = 1.2$. The interference between the modes of the two surfaces depends on the film thickness L. For small values of L, their splitting into two bands is clear. As the film thickness increases, the difference between the modes becomes negligible.

In figure 7 and figure 8 we plot power spectra as functions of the distance to the surface. In figure 7 we have the surface modes in a thin film with $L = 0.1$. Here $Q_y = 6$ and $\omega = 1.001$. This corresponds to a situation where the surface energy is quite high, and decreases as one moves from the interface to the film. Finally, in figure 8 we have $Q_y = 7.5$ and $\omega = 0.9986$, which corresponds to $\mu \approx 22$, and, consequently, to the region of the volume-localized (guided) modes. The film has thickness $L = 5$, which is larger than the mode wavelength. We see oscillations in the power spectrum. These oscillations decay as we get deeper into the film.

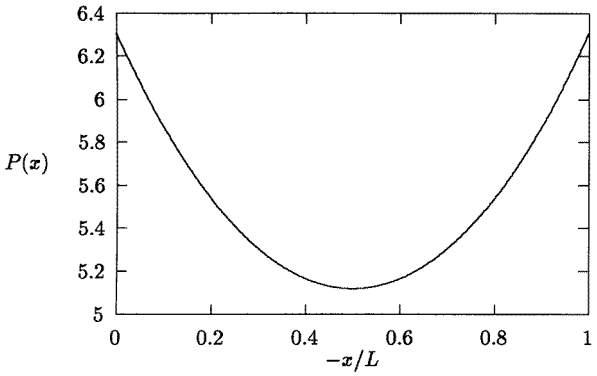

Figure 7. The power spectrum as a function of the distance to the surface for a thin film. Here $L = 0.1$, $Q_y = 6$, $\omega = 1.00135 -$ curve (b) of figure 3. We observe that in the middle of the film, P is at its minimum.

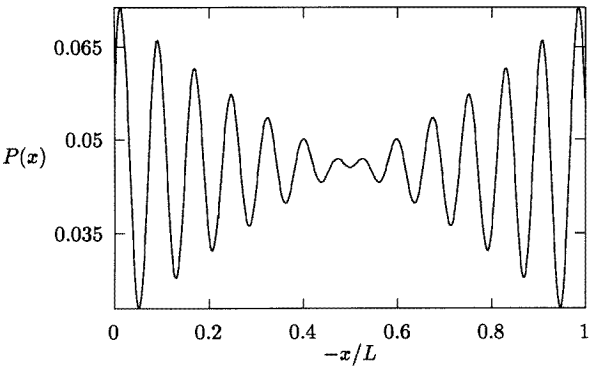

Figure 8. The power spectrum of the volume-localized (guide) modes, as a function of the distance to the surface for a thick film. Here $L = 5$, $Q_y = 7.5$, $\omega = 0.9986$. The oscillatory character due to the surface decays into the volume. The surfaces induce oscillations similar to those of a point charge in an electron gas (Friedel oscillations).

5. Conclusions

In summary, we have used a very simple procedure to build up the Green's functions for the elementary magnetic excitations in thin films, starting from those of a single interface. The main idea is to transform the boundary condition into a virtual potential, and to associate it with the single-surface propagator, so that we can make a diagrammatic expansion. The final Green's functions are the bare Green's functions for a simple propagator (that is, ones whose trajectories going from x' to x do not include closed trajectories), screened by a generalized dielectric function $\sigma(Q_y, \omega)$. The generalized dielectric function is the inverse of the sum of all of the closed trajectories. So, the resulting Green's functions can be seen as the sum of the 'dressed' (the bare ones divided by σ) Green's functions. This process is analogous with the screening process in electron gas [8, 15, 16].

We verified that the Green's function obtained by our method agrees with some results found in the literature obtained by direct calculations. The Green's functions also have an exchange symmetry. With the Green's functions, we obtain the dispersion relation and

the power spectra. We demonstrated specific applications to MnF_2 film at zero field. This crystalline film has the advantage of being easily found in most of laboratories investigating magnetism.

The question remains of how one can possibly obtain negative numbers for the power spectrum, which should only have positive values. Putting this another way, we are asking in what sense equation (29) is different from the following density of states:

$$\rho(E) = \sum_i \delta(E - E_i). \tag{30}$$

Here, E_i is the energy of the state i. We are not going to give a final answer to this question. However, we shall point out the main differences. Equation (29) is far more complex than equation (30). It requires the existence of thermal excitations distributed among the accessible states. Also, the system must be close to equilibrium, and the response must be linear. These are far more restrictive conditions than those that apply to equation (30). Being far from equilibrium means being far from the region of existence of stable modes, and we cannot apply the fluctuation-dissipation theorem without equation (29) having to be modified. So, getting a negative power spectrum indicates that such excitations should not exist in that region—that is, they are unstable.

This diagrammatic method may be applied to different kinds of excitation and different problems of surface science. We think it highly likely that similar processes could be used in different areas of physics. We hope that this work will constitute a first step in the direction of more general and simple methods. An attempt to generalize this result in order to include complex layered structures and surface disorder is being made.

Acknowledgments

This work was supported by CNPq and FINEP (Brazil). One of us, SPD, would like to thank the CNPq for a scholarship awarded during the realization of this work.

References

[1] Hartstein A, Burstein E, Maradudin A A, Brewer R and Wallis R F 1973 *J. Phys. C: Solid State Phys.* **6** 1266
[2] Karsono A D and Tilley D R 1978 *J. Phys. C: Solid State Phys.* **11** 3487
[3] Camley R E and Mills D L 1982 *Phys. Rev.* B **26** 1280
[4] Fukui M, Dohi H, Matsuura J and Toda O 1984 *J. Phys. C: Solid State Phys.* **17** 1783
[5] Lima N P and Oliveira F A 1983 *Solid State Commun.* **47** 921
[6] Oliveira F A, Lima N P and dos Santos A R 1987 *Mod. Phys. Lett.* B **1** 129
[7] Oliveira F A 1993 *Solid State Commun.* **85** 1051
[8] Matuck R D 1976 *A Guide to Feynman Diagrams in the Many-Body Problem* (New York: Dover)
[9] Dobrzynski L 1987 *Surf. Sci.* **182** 362
[10] Sarmento E F and Tilley D R 1976 *J. Phys. C: Solid State Phys.* **9** 2943
[11] Maradudin A A and Zierau W 1976 *Phys. Rev.* B **14** 484
[12] Stamps R L and Camley R E 1989 *Phys. Rev.* B **40** 609
[13] Lima N P and Oliveira F A 1986 *J. Phys. C: Solid State Phys.* **19** 5381
[14] Oliveira F A, Cottam M G and Tilley D R 1981 *Phys. Status Solidi* b **107** 737
[15] Garavelli S L and Oliveira F A 1991 *Phys. Rev. Lett.* **66** 1310
[16] Garavelli S L and Oliveira F A 1992 *Mod. Phys. Lett.* B **6** 811
[17] Kliewer K L and Fuchs R 1966 *Phys. Rev.* **144** 495
[18] Loudon R 1978 *J. Phys. C: Solid State Phys.* **11** 2623
[19] Moul R C and Cottam M G 1983 *J. Phys. C: Solid State Phys.* **16** 1784
[20] dos Santos A R and Cottam M G 1982 *Proc. 7th Int. Conf. on Raman Spectroscopy* (Amsterdam: North-Holland) p 98
[21] Marchand M and Caillé A 1980 *Solid State Commun.* **34** 827

[22] Oliveira F A 1981 *Solid State Commun.* **40** 859
[23] Cottam M G and Tilley D R 1989 *Introduction to Surface and Superlattice Excitations* (Cambridge: Cambridge University Press)
[24] Agranovich V and Maradudin A A 1984 *Surface Excitations* (Amsterdam: North-Holland)
[25] Tilley D R 1980 *J. Phys. C: Solid State Phys.* **13** 781